ELSEVIER Nuclear Instruments and Methods in Physics Research B 175–177 (2001) 468–473

NIM B
Beam Interactions with Materials & Atoms

www.elsevier.nl/locate/nimb

Formation of Ge nanowires in oxidized silicon V-grooves by ion beam synthesis

T. Müller *, K.-H. Heinig, B. Schmidt

Forschungszentrum Rossendorf, Institut für Ionstrahlphysik und Materialforschung, P.O. Box 51 01 19, 01314 Dresden, Germany

Abstract

The formation of Ge nanowires in V-grooves on (0 0 1)Si wafers has been studied experimentally as well as theoretically. The V-grooves were formed by anisotropic etching and subsequent oxidation of their surface. The implantation of 1×10^{17} Ge^+ cm^{-2} at 70 keV into the oxide layer leads to an enrichment of Ge in the V-groove bottom. In this Ge-rich bottom region, subsequent annealing in N_2 atmosphere results in the formation of a nanowire by coalescence of Ge precipitates. Scanning transmission electron microscopy-energy dispersive X-ray analysis (STEM-EDX) investigations of as-implanted samples have confirmed the Ge accumulation at the V-groove bottom, whereas cross-sectional TEM studies of annealed samples prove the formation of a Ge nanowire. The formation mechanisms were studied theoretically by means of a continuum description of sputtering and kinetic 3D lattice Monte-Carlo simulations of phase separation. The preliminary results indicate the possibility of achieving nanowires being several nanometers wide by further growth optimizations. © 2001 Elsevier Science B.V. All rights reserved.

PACS: 61.72.Ss; 68.65.+g; 85.30.Vw
Keywords: Ion beam synthesis; Nanowire; V-groove; Coalescence

1. Introduction

Low-dimensional nanostructures have attracted much interest in the past. In particular, ion beam synthesis (IBS) became successful for a controlled synthesis of buried nanostructures. Thus, quantum dots were formed by IBS under various conditions [1,2]. Using very high ion fluences, buried layers are synthesized [3]. During thermal treatment, the supersaturated solid solution of impurities produced by ion implantation evolves towards nanostructures by precipitation and growth, and by coalescence for high concentrations. Although not obvious, these inherently stochastic processes can be used to synthesize well-defined nanostructures. The aim of the present paper is to form Ge nanowires by IBS. An interesting method of IBS of Si nanowires has recently been demonstrated by O^+ implantation into Si V-grooves [4]. However, this method appears to rely strongly on sensitive self-organization phenomena during Ostwald-ripening, which allows no precise process control. Here, we propose the most direct

* Corresponding author. Tel.: +49-351-260-3148; fax: +49-351-260-3285.
E-mail address: t.mueller@fz-rossendorf.de (T. Müller).

0168-583X/01/$ - see front matter © 2001 Elsevier Science B.V. All rights reserved.
PII: S0168-583X(00)00673-X

way of IBS of nanowires using V-grooves. The key is the tailoring of the profile of implanted impurities, which will coalesce to a wire.

For this purpose, (0 0 1)Si wafers with oxidized V-grooves were implanted with Ge^+ ions. The scheme is depicted in Fig. 1. Let us assume that at plane surfaces the implanted ion fluence is just sufficient to form a continuous buried layer. In the slanted V-groove sidewalls the number of implanted ions per unit area is lower than at the plane wafer surface. This reduced Ge concentration will be too low to allow an efficient coalescence of precipitates, which is the crucial process for the layer formation. However, at the V-groove bottom the concentration is expected to be high enough to allow coalescence, since the bottom can be considered as a small plane area. Additionally, the efficient sputtering of atoms from the V-groove sidewalls and the redeposition of these sputtered atoms onto the opposite V-groove sidewall leads to material transport into the bottom region, which has been modelled recently in a continuum picture [5]. An effective Ge accumulation at the V-groove bottom is proven by 2D Ge mapping with scanning transmission electron microscopy-energy dispersive X-ray analysis (STEM-EDX). During subsequent annealing, this accumulation has led to the formation of a buried nanowire, which is shown by cross-sectional transmission electron microscopy (XTEM), identifying a diameter of 35 nm.

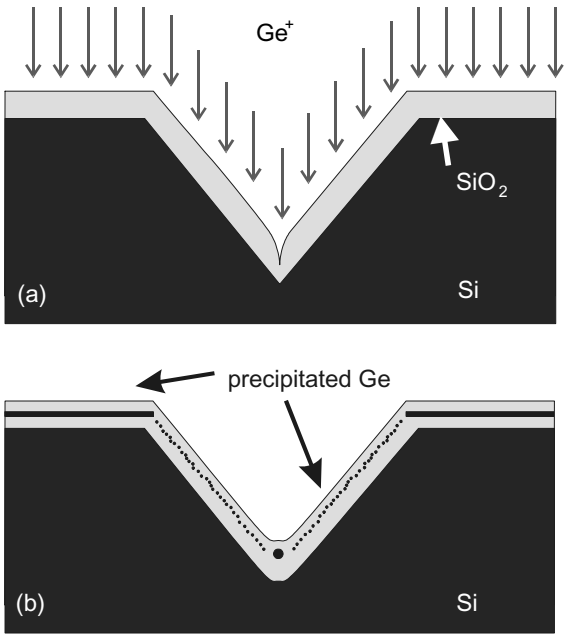

Fig. 1. Scheme of IBS of a buried Ge nanowire in the bottom of an oxidized silicon V-groove. (a) Ge^+ will be implanted at high fluence into SiO_2 covered silicon V-grooves and (b) the sample will be subsequently annealed in an inert ambient.

The growth has been studied theoretically by means of kinetic 3D lattice Monte-Carlo (KLMC) simulations allowing a better understanding of the underlying phase separation mechanism.

2. Experimental

V-grooves aligned along the [1 1 0] direction on (0 0 1)Si wafers were prepared by photolithographic masking and anisotropic etching with 30% KOH at 80°C. This self-adjusting process results in atomically smooth (1 1 1) crystal facets forming the sidewalls of the V-grooves and with an angle of 54.7° to the surface normal of the wafer. V-grooves of 4 μm width and 5 nm length were studied. Thermal oxidation in dry O_2 was performed at 1000°C, leading to 200 nm thick SiO_2 on the (0 0 1)Si surface and 220 nm thick SiO_2 on the (1 1 1) sidewalls of the V-groove. A sharp surface depression forms at the V-groove bottom during oxidation (Fig. 2(a)). The SiO_2 covered V-grooves were implanted at room temperature with 1×10^{17} Ge^+ cm^{-2} at 70 keV (flux density 3×10^{12} cm^{-2} s^{-1}). Subsequent annealing was carried out in N_2 ambient at 950°C for 10 min. In order to minimize the moisture intake, the sample was transferred into the cold furnace.

XTEM images were taken from as-oxidized, as-implanted, and annealed samples, shown in Figs. 2 and 4. Additionally, using STEM-EDX, a 2D Ge mapping of an as-implanted sample was performed, which is shown in Fig. 3.

3. Kinetic Monte-Carlo simulation

Naturally, the most appropriate theoretical method to study the wire formation from an

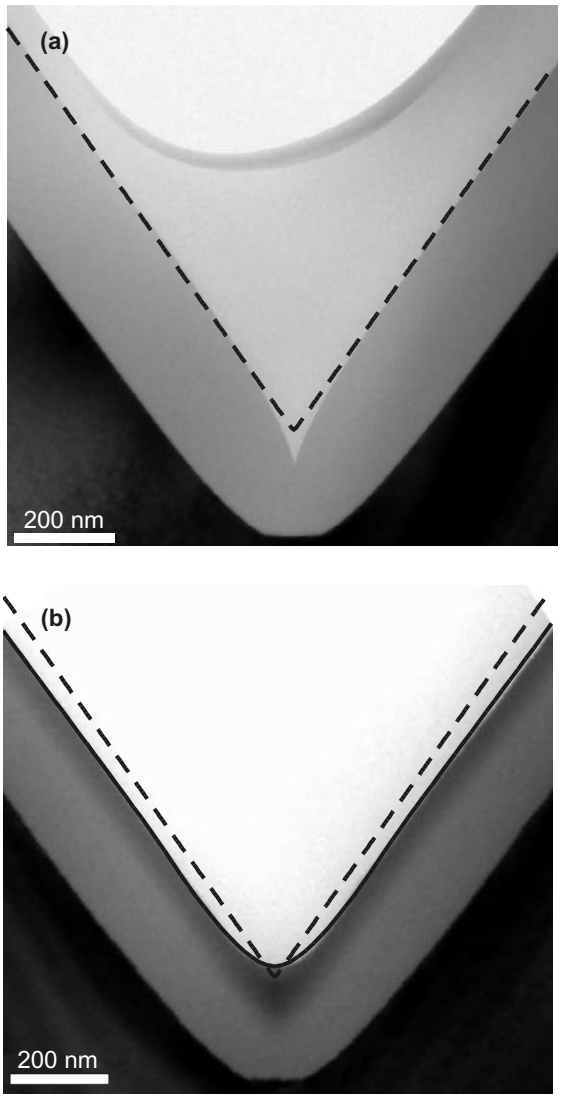

Fig. 2. XTEM images of (a) an as-oxidized state and (b) an as-implanted sample (70 keV, 1×10^{17} Ge^{+} cm^{-2}). The dashed line indicates the idealized location of the original, not implanted V-groove. The solid curve is the surface after ion implantation as predicted by the theory of [5], which agrees nicely with the XTEM image (Fig. 2(b)).

inhomogeneous supersaturation is an atomic description. For processes with many degrees of freedom, statistical Monte-Carlo methods are advantageous compared to deterministic molecular dynamics simulations. Here, a KLMC code for diffusion and reaction of impurity atoms on a 3D fcc lattice has been used. In order to keep simulation time below one week, the system of the computer simulation is still smaller than the system studied experimentally. A general description of the KLMC method can be found in [6].

Here, interactions between impurity atoms (Ge) were simulated by a cellular automation approach (see e.g. [7]). Gauging the binding energy per bond E_B of the impurity atoms, their effective nearest-neighbor interactions within the host matrix has been considered. Here, the most simple implementation is used, i.e., the interaction is assumed to be independent of the occupation of nearest-neighbor Ge sites. The binding energy nE_B is just proportional to the number of occupied nearest-neighbor Ge sites n and can be described by the Ising model [7]. Additionally, the diffusion of monomers in the host matrix is thermally activated with an activation energy E_A.

Then, the transition from the initial out-of-equilibrium state towards the thermodynamical equilibrium is described by a Markov process, where the importance sampling of configurations have been chosen according the Metropolis algorithm [8]. A sequence of states is produced representing the time evolution. Each state is generated from its predecessor by a jump of a randomly chosen atom to a neighboring empty site with a the transition probability

$$P_{\mathrm{if}} = \begin{cases} \exp\left\{-\frac{E_A}{k_B T}\right\}, & n_f \geqslant n_i, \\ \exp\left\{-(n_i - n_f)\frac{E_B}{k_B T} - \frac{E_A}{k_B T}\right\}, & n_f < n_i. \end{cases}$$

During one Monte-Carlo step (MCS), each atom has statistically one attempt to jump from its initial site i to the final site f. The principle of detailed balance imposes only that the transition probability P_{if} depends on the energy barrier between the initial and final state. It is possible to renormalize the transition probability P_{if} such that each diffusional jump is successful $(E_A \to 0)$, which scales only the time of a MCS but improves the simulation speed,

$$P_{\mathrm{if}} = \begin{cases} 1, & n_f \geqslant n_i, \\ \exp\left\{-(n_i - n_f)\frac{E_B}{k_B T}\right\}, & n_f < n_i. \end{cases}$$

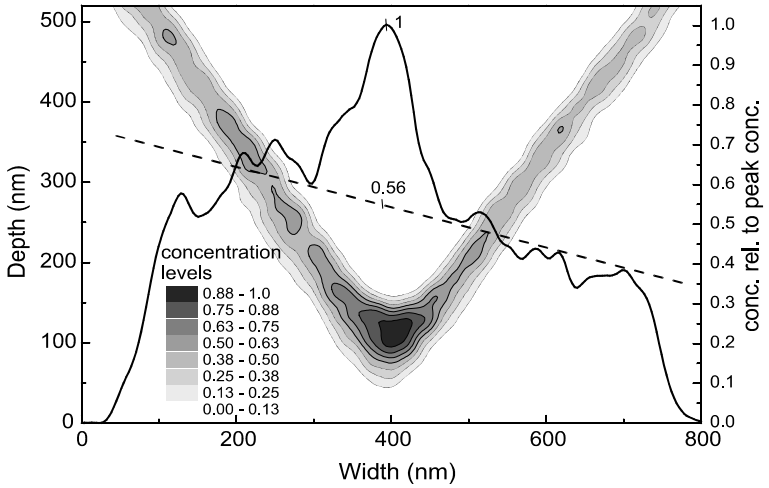

Fig. 3. STEM-EDX Ge mapping on a cross-section of an as-implanted sample. The levels of gray correspond to the concentration of Ge relative to the maximum concentration of 30 at.% in the V-groove bottom. The solid curve shown is the projection of the Ge concentration onto the horizontal axis. The average Ge content in the sidewalls is shown by a dashed line, which discriminates the Ge enriched bottom from the sidewalls.

This approach has been proven useful for the description of precipitation after ion implantation [9]. For the KLMC simulation of the nanowire formation a simplified initial impurity distribution was assumed. A cylindrical Gaussian profile aligned to the [1 0 0] direction of the simulation lattice was used as shown in Fig. 5(a). A peak concentration of 31% and a standard deviation of 4 nm was assumed. 95% of the implanted atoms lay in a cylinder of 16 nm diameter, which resembles the Ge-rich region at the bottom of the V-groove.

4. Results and discussion

High-fluence Ge^+ implantation erodes the SiO_2 on V-groove sidewalls and leads to an accumulation of material (Si, O, Ge) at the V-groove bottom. This effect is shown in Fig. 2, comparing XTEM images of as-oxidized and as-implanted samples. The sharp depression of the as-oxidized surface at the V-groove bottom is refilled during implantation by sputtered and then redeposited material, which has been simulated recently [5] and is shown in Fig. 2(b) as solid line. The model uses a continuum description for the surface evolution under ion irradiation, including sputtering and redeposition of sputtered atoms. The material accumulated at the V-groove bottom is enriched by Ge, which is confirmed by the STEM-EDX mapping in a cross-section of an as-implanted sample (Fig. 3). Due to a slight wedge in the specimen, the concentration profile is asymmetric with respect to the center of the V-groove. The left side is thicker than the right one resulting in an increased X-ray yield there. Both the Ge concentration (~30%) and the total amount of Ge are in the V-groove bottom much higher than in the sidewalls. The total amount is estimated from the projection of the concentration profile onto the x-axis, which is shown as a solid curve in Fig. 3.

During subsequent annealing, the Ge accumulated in the V-groove bottom forms a wire by precipitation and coalescence, while the threshold for coalescence is not reached in the sidewalls and only nanoclusters are formed there. Fig. 4 shows a XTEM image of an annealed sample. Buried Ge clusters are present in the sidewalls and the bottom. The dark dot, visible in the V-groove bottom, is a cross-section of the expected nanowire with a diameter of 35 nm. The continuity of the wire remains to be proven,

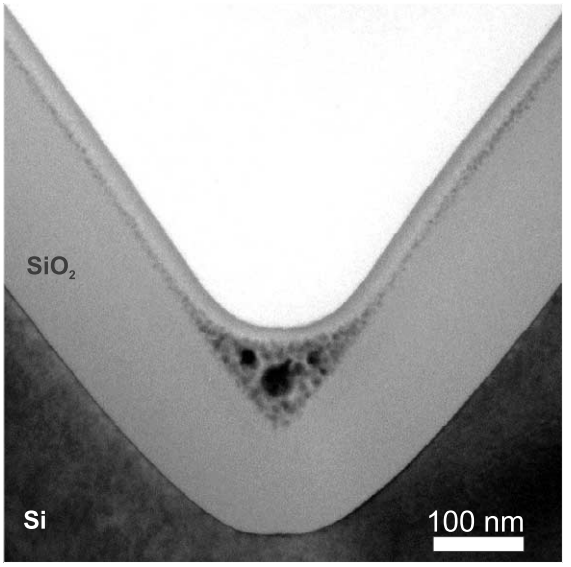

Fig. 4. XTEM image of an annealed sample. Ge cluster in the SiO_2 layer appear dark. The large cluster in the V-groove bottom is a cross-section of the Ge nanowire with 35 nm diameter.

since a plane view TEM image is still missing. Nevertheless, several XTEM images taken from different cross-sections show always the large black dot with identical diameter in the bottom of the V-groove, which is at least a strong indication for a continuous nanowire. Furthermore, it can be seen that the first 20 nm below the SiO_2 surface are free of Ge clusters and appear brighter. This range was affected by moisture from the ambient leading to Ge oxidation and redistribution processes, which have been described recently in [2]. Obviously, the nanowire has not been affected, since it is buried deeper than 20 nm in the SiO_2. It should be noted that oxidation suppresses the formation of Ge clusters in the sidewalls.

Using KLMC simulations, some aspects of the wire formation mechanism can be understood without an immense experimental effort. Fig. 5 shows as an example the simulation of the synthesis of a 6 nm thin nanowire from an initially cylindrical Gaussian profile. The dispensed impurity atoms literally condense onto the profile center. In detail, this process consists of different steps: the nucleation stage, the competitive growth of Ge clusters (Ostwald-ripening), and their coalescence. Complete coalescence will only occur, if the initial profile is not too broad or the Ge concentration not too low. Otherwise, the clusters remain isolated, in the course of coarsening they do not reach the percolation threshold for coalescence. On the other side, during further annealing, a continuous wire is metastable only, since a set of large clusters has a smaller surface area and, thus, is energetically favored. Due to thermal fluctuations especially thin wires can be fragmented into droplets. Additionally, being aligned to the [1 0 0] direction, the simulated wire has (1 0 0) surfaces, which have a higher surface energy than (1 1 1) surfaces. The evolution of energetically favored (1 1 1) facets on the wire surface may act as a knife and directly lead to the fragmentation of the wire. In contrast, wires aligned to the [1 1 0] direction having (1 1 1) facets would be relatively stable at much smaller diameters. Thus, the wire stability depends on the relative alignment of the single crystalline wire to the simulation lattice. However, an experimentally synthesized wire in an amorphous matrix, i.e. SiO_2, should rather be polycrystalline. Here, grain boundaries may provide a source of instability against a breakup. Thus, Fig. 5 gives a realistic estimate of the reachable wire diameter, which is approximately 5–10 nm. Beside this instability considerations, the KLMC simulations give an indication that temperature variation during phase separation allows to take additional control over the nanostructure synthesis. The background is that nucleation and cluster growth have different activation energies, and a change in temperature will favor different processes at specific stages of the evolution.

In summary, IBS was used to fabricate Ge nanowires embedded in SiO_2. It has been shown experimentally that (i) Ge^+ implantation into oxidized silicon V-grooves leads to Ge accumulation in the V-groove bottom and that (ii) wires can be formed from this enriched Ge during annealing. A Ge wire of 35 nm diameter has been found. Kinetic Monte-Carlo simulations were used to estimate a lower limit for the wire diameter (5–10 nm) and show the instability of the wire against a possible breakup.

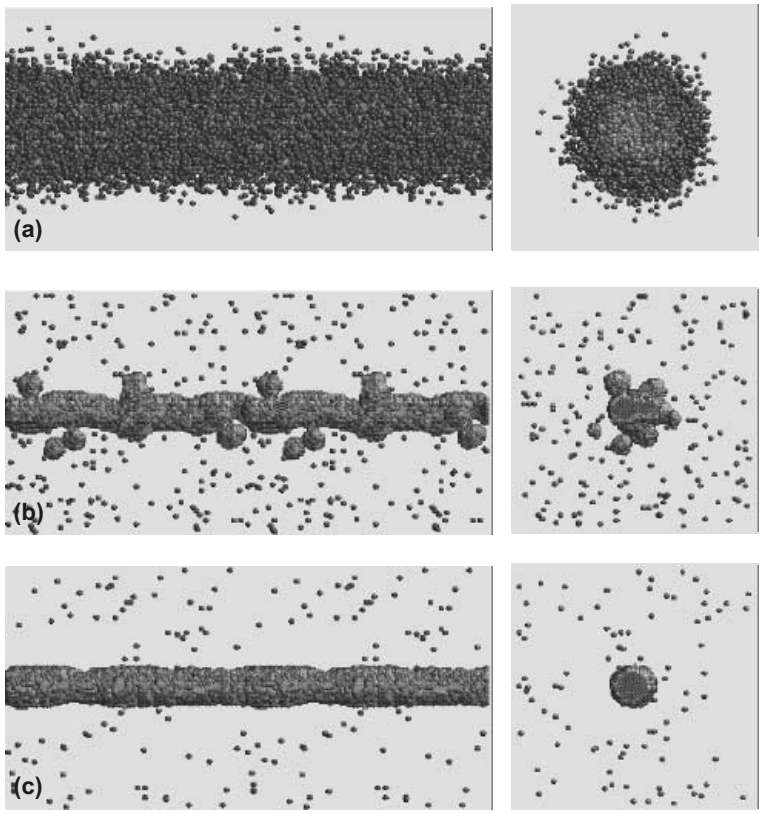

Fig. 5. KLMC simulation of the nanowire formation from an initially cylindrical Gaussian profile with a peak concentration of 31% and a standard deviation of 4 nm. Shown are (a) the initial, (b) an intermediate (102 000 Monte-Carlo steps) and (c) the final (490 000 Monte-Carlo steps) state. The wire diameter is approximately 5 nm.

Acknowledgements

We gratefully wish to acknowledge the help of Arndt Mücklich in taking the EDX mapping and Prof. Möller for his steady and strong encouragement.

References

[1] C.W. White, J.D. Budai, S.P. Withrow, J.G. Zhu, S.J. Pennycook, R.A. Zuhr, D.M. Hembree Jr., D.O. Henderson, R.H. Magruder, M.J. Yacaman, G. Mondragon, S. Prawer, Nucl. Instr. and Meth. B 127/128 (1997) 545.
[2] K.-H. Heinig, B. Schmidt, A. Markwitz, R. Grötzschel, M. Strobel, S. Oswald, Nucl. Intstr. and Meth. B 148 (1999) 969.
[3] Y. Li, C.D. Marsh, A. Nejim, R.J. Chater, J.A. Kilner, P.L.F. Hemment, Nucl. Instr. and Meth. B 99 (1995) 479.
[4] Y. Ishikawa, N. Shibata, S. Fukatsu, Nucl. Instr. and Meth. B 147 (1999) 304.
[5] T. Müller, K.-H. Heinig, B. Schmidt, Nucl. Instr. and Meth. B 179 (2001) in press.
[6] M.E.J. Newman, G.T. Barkema, in: Monte Carlo Methods in Statistical Physics, Oxford University Press, Oxford, 1999.
[7] J. Schmelzer, G. Roepke, R. Mahnke, in: Aggregation Phenomena in Complex Systems, Wiley, New York, 1999.
[8] N. Metropolis, A. Rosenbluth, M. Rosenbluth, A. Teller, E. Teller, J. Chem. Phys. 21 (1953) 1087.
[9] M. Strobel, K.-H. Heinig, W. Möller, Comput. Mater. Sci. 10 (1998) 457.